



*Supplement of*

**Global warming will largely increase waste treatment CH<sub>4</sub> emissions in Chinese megacities: insight from the first city-scale CH<sub>4</sub> concentration observation network in Hangzhou, China**

Cheng Hu et al.

*Correspondence to:* Bing Qi (bill\_129@sina.com) and Rongguang Du (drg1998@163.com)

The copyright of individual parts of the supplement might differ from the article licence.

### **Section S1. Choice of CH<sub>4</sub> background based on monthly footprint**

We carefully choose the CH<sub>4</sub> background for each month by identifying the main air flows based on monthly footprint (Figure S3). The final choice is displayed in Table S2. And we should note because the difference between YON and other four sites of TAP, RYO, WLG and UUM sites were larger as 100 ppb from May to August, which indicates there is large uncertainty when air flows come from directions of both YON site and other four sites. We found the footprint in July showed obvious air follows both from the South China Sea (YON site) and north east of observation site (RYO site), and to reduce the potential large uncertainty in CH<sub>4</sub> simulations, we used the averages of both sites as the background in July.

### **Section S2. Multiplicative scaling factor method**

We also used the multiplicative scaling factor (hereafter MSF) method to constrain emissions by using observations at Linan site, which has been applied broadly to constrain greenhouse gas and other tracer gas emissions. The MSF SFs were derived by dividing the observed enhancement by the simulated enhancement (Sargent et al., 2018; He et al., 2020),

$$SF(CH_4) = \frac{CH_{4\_obs} - CH_{4\_bg} - \Delta CH_{4\_wetland}}{\Delta CH_{4\_anthro}} \quad (3)$$

where SF(CH<sub>4</sub>) is the scaling factor for anthropogenic CH<sub>4</sub> emissions (excluding agricultural soil in this study), and CH<sub>4\_obs</sub>, CH<sub>4\_bg</sub>, ΔCH<sub>4\_wetland</sub> and ΔCH<sub>4\_anthro</sub> are the CH<sub>4</sub> concentration observations, background CH<sub>4</sub>, simulated wetland CH<sub>4</sub> enhancement, and simulated anthropogenic CH<sub>4</sub> enhancement (excluding agricultural soil), respectively.

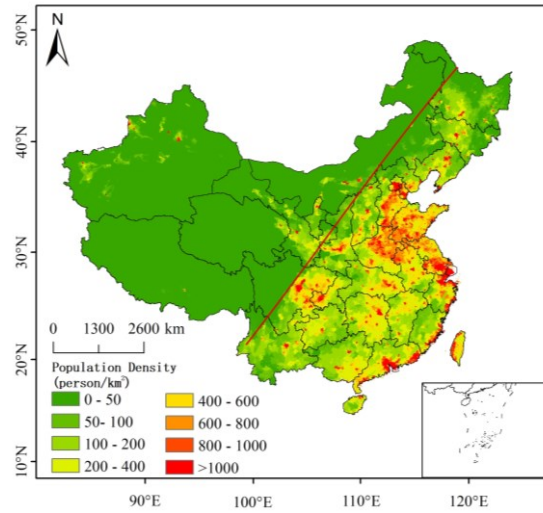


Figure S1. Population density for China in year of 2019, with the red line represents Heihe-Tengchong line, with 94% of national total population lived in the east of this line.

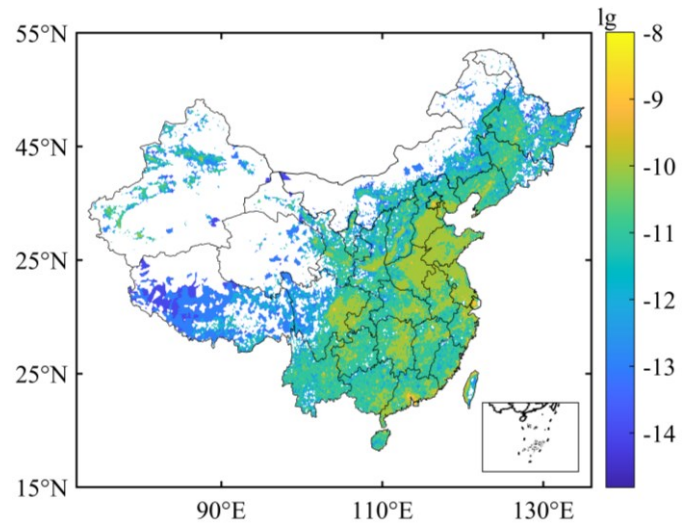


Figure S2. Waste treatment CH<sub>4</sub> emissions in EDGAR v6.0 inventory, units for emissions: kg m<sup>-2</sup> s<sup>-1</sup>.

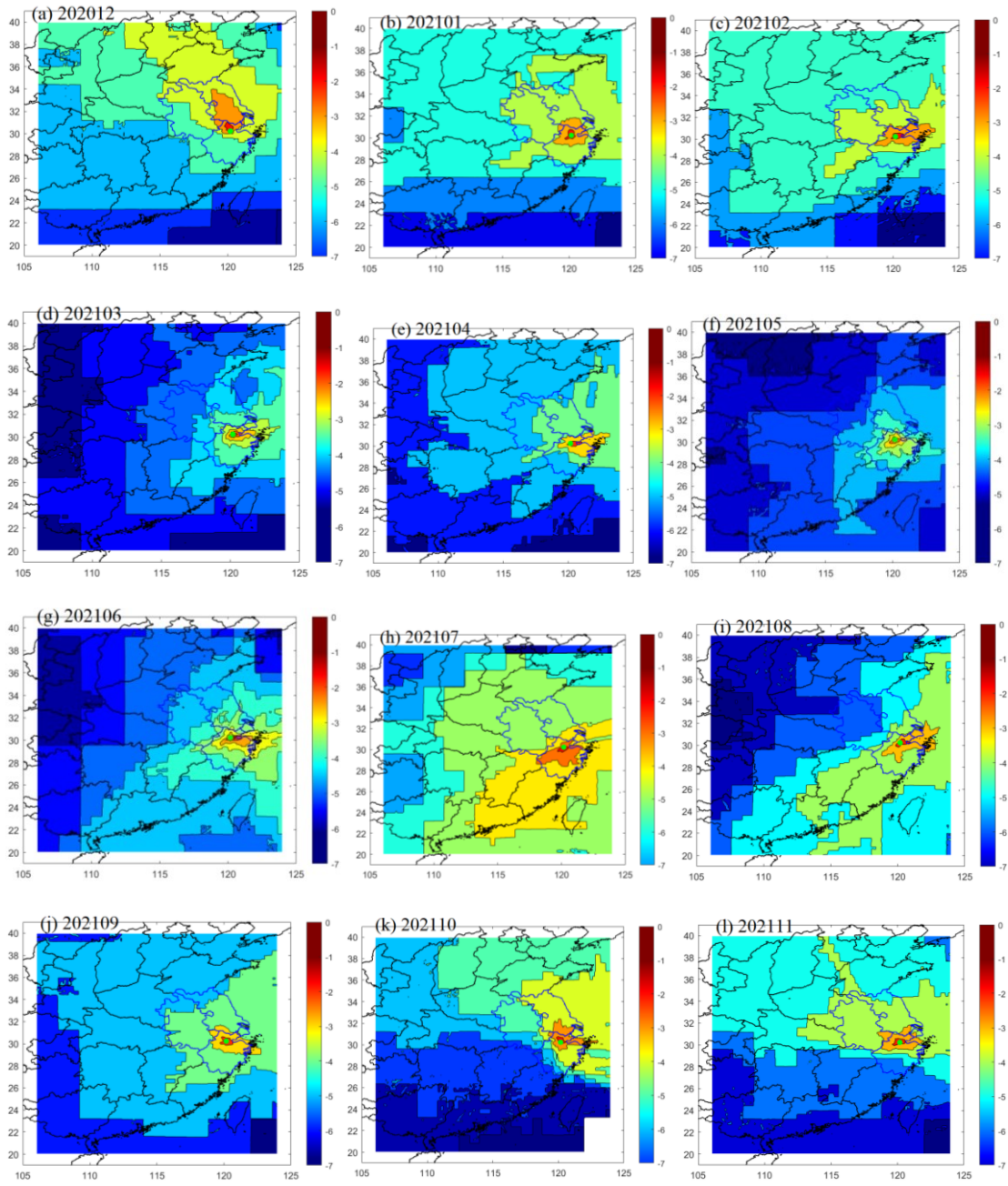


Figure S3. Monthly averaged footprint from December, 2020 to November, 2021, units for footprint:  $\text{ppm m}^2 \text{s mol}^{-1}$ .

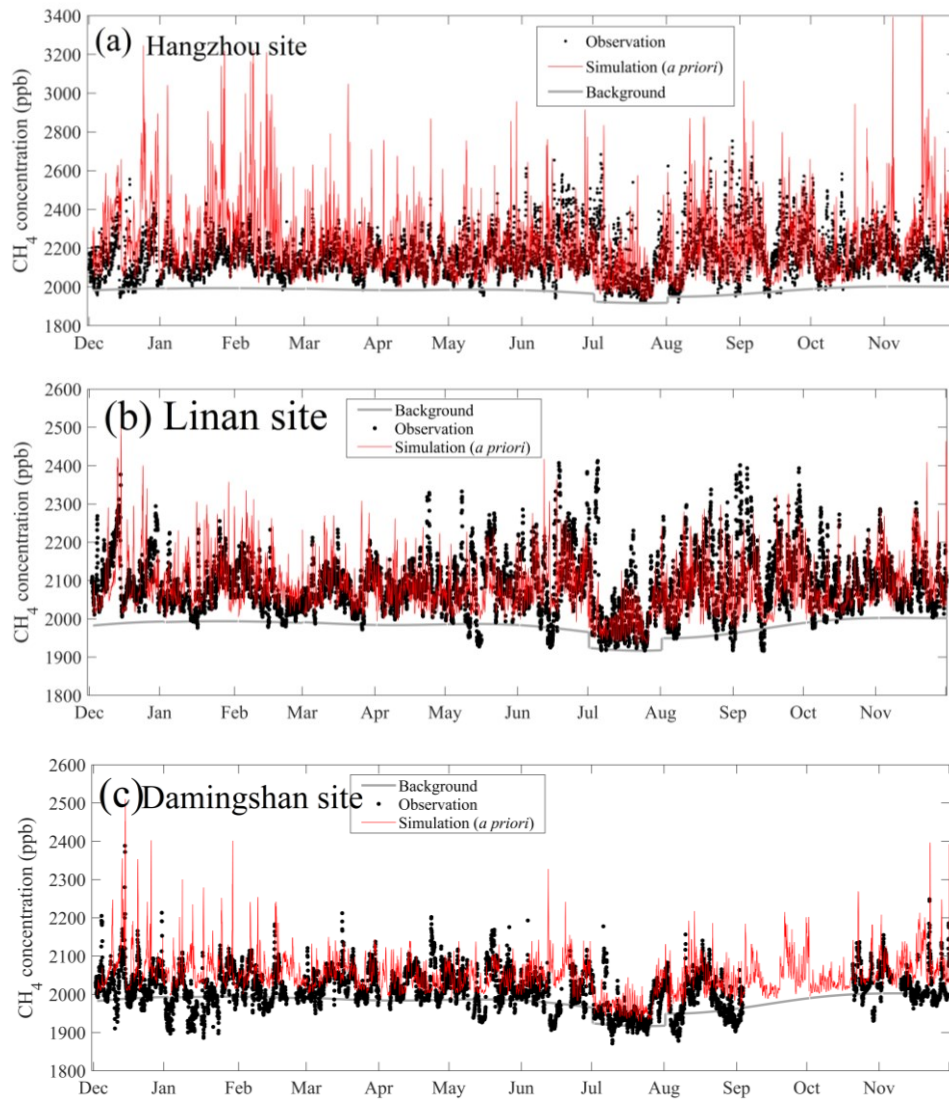


Figure S4. Comparisons between hourly CH<sub>4</sub> concentration simulations and observations at three sites.

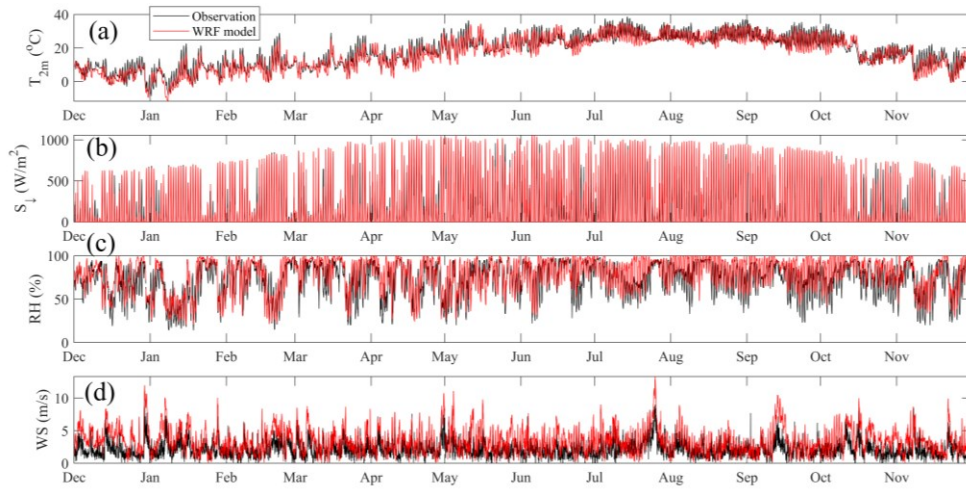


Figure S5. Comparisons between observed and simulated meteorological fields for air temperature at 2 m ( $T_{2m}$ ), relative humidity (RH), downward solar radiation ( $S_{\downarrow}$ ), and wind speed (WS) at 10 m height.

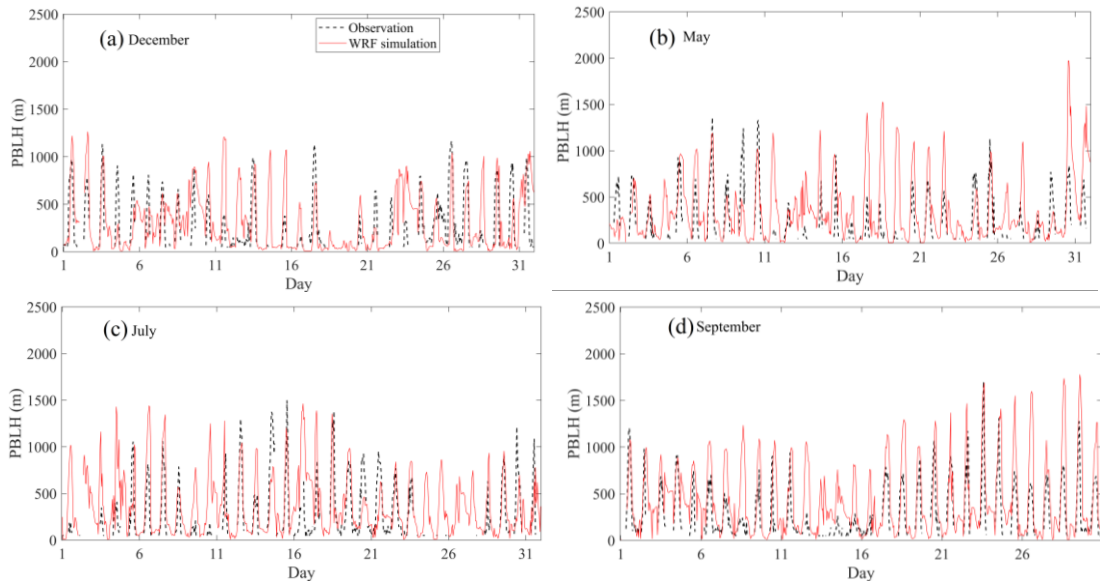


Figure S6. Comparisons between Simulated and observed hourly PBLH in (a) December 2020, (b) May 2021, (c) July 2021, and (d) September 2021.



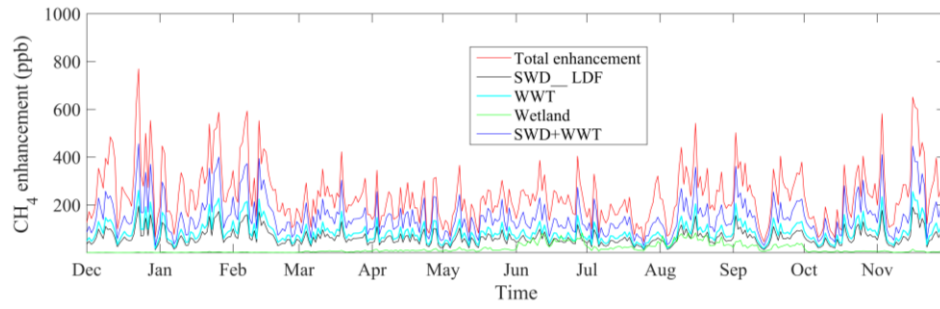


Figure S7. Daily variations of simulated CH<sub>4</sub> enhancements from different categories for Hangzhou site.

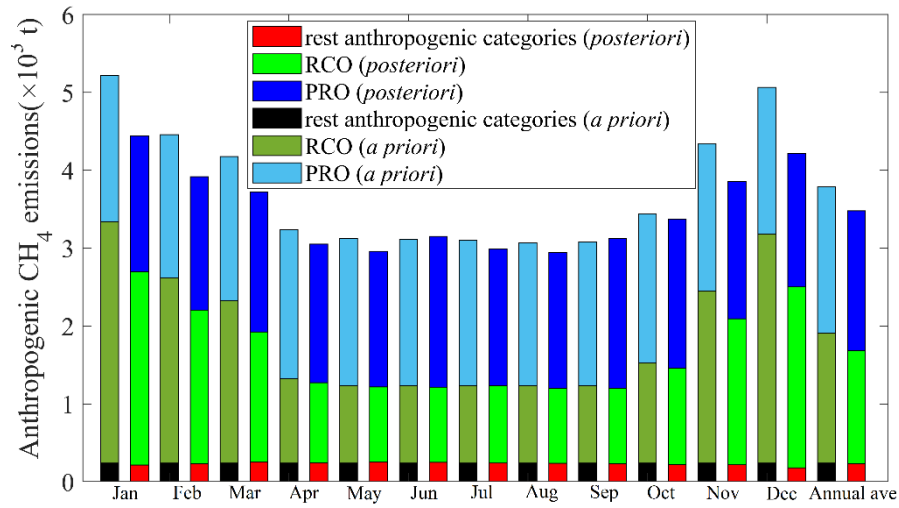


Figure S8. Comparisons of anthropogenic CH<sub>4</sub> emissions between *a priori* and *posteriori* results, PRO: fuel exploitation, RCO: energy for building, the rest anthropogenic emissions: excluding waste treatment, PRO, RCO and agricultural soil.

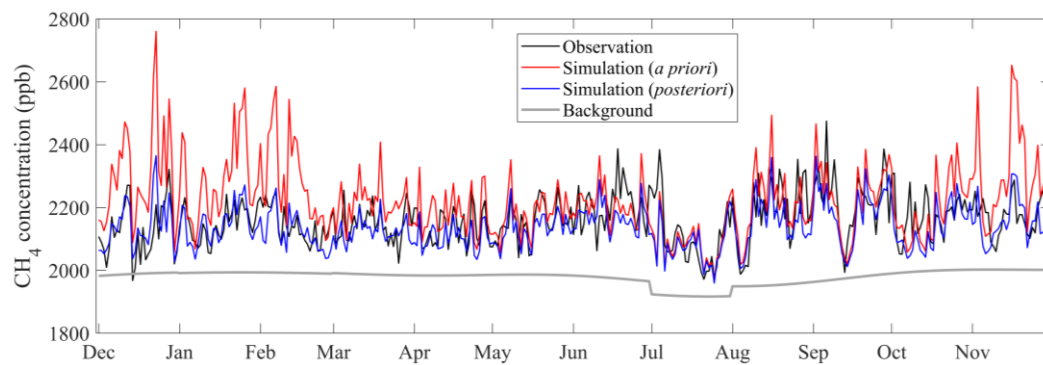


Figure S9. Daily CH<sub>4</sub> concentrations comparisons using both *a priori* and *posteriori* emissions.

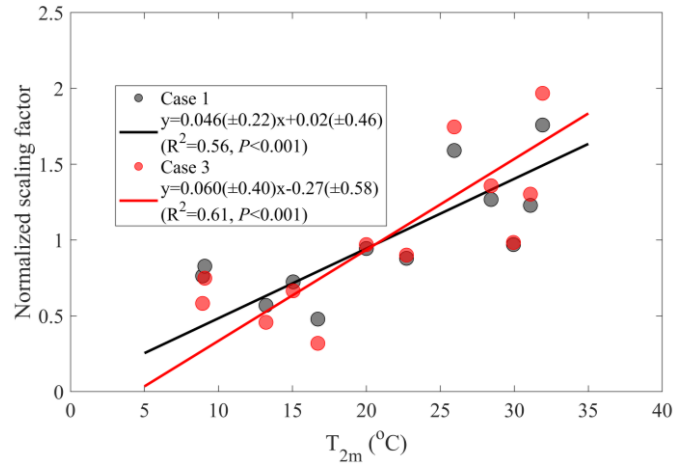


Figure R10. Relationship between the monthly *posteriori* CH<sub>4</sub> emissions and temperature in case 1 and 3.

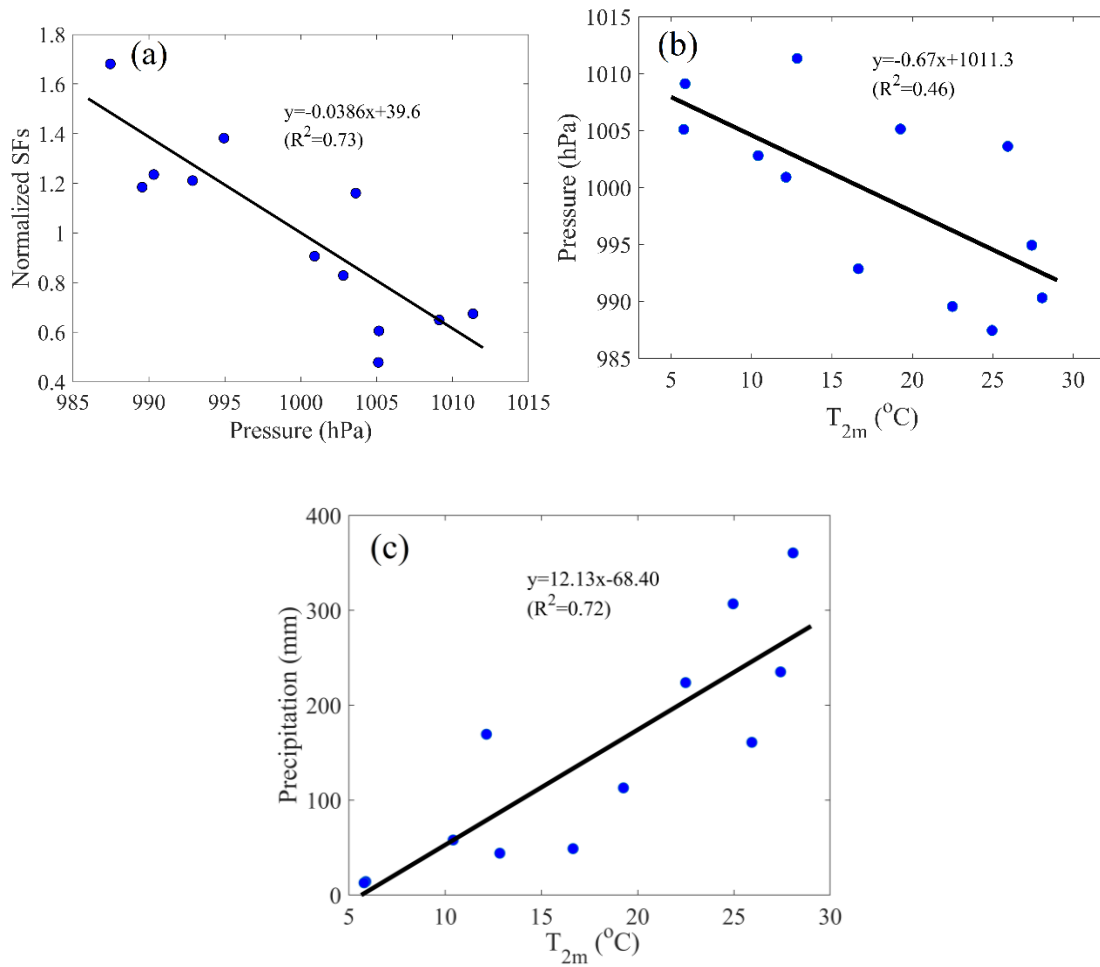


Figure S11. (a) Relationship between monthly averaged atmospheric pressure and normalized SFs, (b) relationship between monthly averaged atmospheric pressure and  $T_{2m}$ , and (c) relationship between monthly precipitation and  $T_{2m}$ .

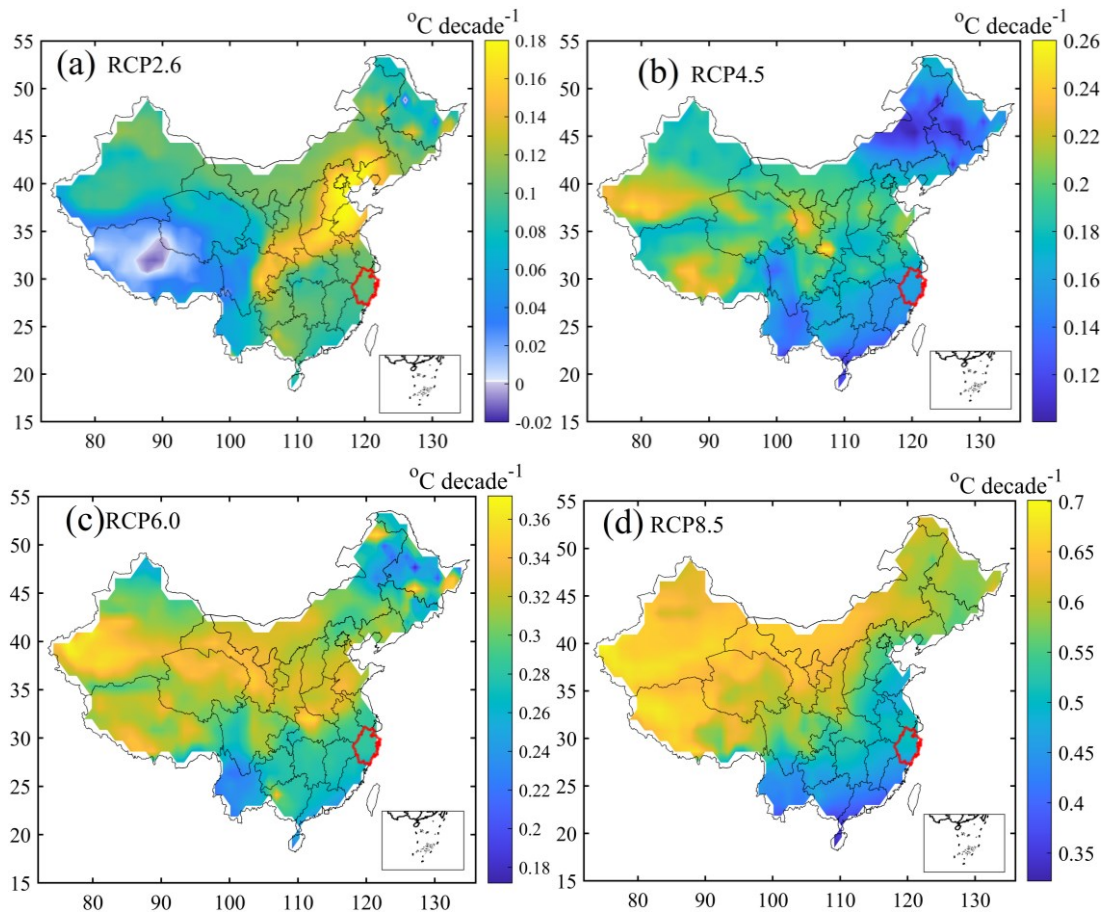


Figure S12. Spatial distributions of air temperature trends in China for (a) RCP2.6, (b) RCP4.5, (c) RCP6.0, and (d) RCP8.5 scenarios. Note the red boundary is Zhejiang province, and the trends represents years from 2020 to 2100.

Table S1. The choice of CH<sub>4</sub> background based on simulated monthly footprint, ‘Y’ indicates concentration at this background site (or averages of both) will be used as CH<sub>4</sub> background for this month.

Sites	Dec	Jan	Feb	Mar	Apr	May	Jun	Jul	Aug	Sep	Oct	Nov
TAP												
YON								Y				
RYO		Y	Y	Y	Y	Y	Y	Y	Y	Y	Y	Y
WLG												
UUM	Y	Y										

Table S2. *Posteriori* Scaling factors by only using daytime (11:00-16:00, local time) observations and simulations.

Month	Case 1			Case 3		
	Wetland	Waste	Others	Wetland	Waste	Others
1	1.00	0.64	0.71	1.00	0.54	0.78
2	1.00	0.44	0.82	1.00	0.33	0.93
3	1.01	0.56	0.98	1.02	0.48	1.06
4	1.12	0.73	1.13	1.13	0.70	1.16
5	1.16	1.23	1.01	1.15	1.26	0.97
6	1.08	0.98	1.18	1.08	0.98	1.18
7	1.04	1.36	1.41	1.01	1.42	1.36
8	1.02	0.95	0.99	1.03	0.94	1.00
9	1.02	0.75	0.97	1.04	0.71	1.01
10	1.08	0.68	1.02	1.08	0.65	1.05
11	1.00	0.37	0.72	1.00	0.23	0.83
12	1.00	0.59	0.66	1.00	0.42	0.74



Table S3. Normalized monthly CH<sub>4</sub> SFs based on annual averages for waste treatment, note we calculate the normalized monthly SFs by dividing monthly SFs by annual averages.

Month	Case 1	Case 2	Case 3	Average( $\pm$ STD)
1	0.59	0.64	0.72	0.65( $\pm$ 0.13)
2	0.40	0.49	0.54	0.48( $\pm$ 0.14)
3	0.79	0.87	0.83	0.83( $\pm$ 0.08)
4	0.93	0.91	0.88	0.91( $\pm$ 0.05)
5	1.25	1.21	1.17	1.21( $\pm$ 0.08)
6	1.19	1.21	1.15	1.18( $\pm$ 0.06)
7	1.78	1.66	1.60	1.68( $\pm$ 0.18)
8	1.25	1.25	1.21	1.24( $\pm$ 0.04)
9	1.43	1.38	1.33	1.38( $\pm$ 0.10)
10	1.21	1.15	1.12	1.16( $\pm$ 0.09)
11	0.55	0.60	0.67	0.61( $\pm$ 0.12)
12	0.63	0.62	0.77	0.67( $\pm$ 0.15)